

## Supplementary Information

### **Synergistic effect of coordinating interface and promoter for enhancing ammonia synthesis activity of Ru@N-C catalyst**

Dongwei Wang,<sup>ab</sup> Zhanwei Ma,<sup>\*a</sup> Farong Gou,<sup>a</sup> and Bin Hu<sup>\*a</sup>

- a.** State Key Laboratory for Oxo Synthesis and Selective Oxidation, Lanzhou Institute of Chemical Physics, Chinese Academy of Sciences, Lanzhou 730000, China
- b.** University of Chinese Academy of Sciences, Beijing 100049, China

## 1. Ru/AC(450) catalyst:

The activated carbon particles treated with nitric acid were placed in an ark and roasted in a tube furnace under argon atmosphere at 450 °C for one hour of a heating rate of 5 °C/min. Then  $\text{Ru}_3(\text{CO})_{12}$  was dissolved in tetrahydrofuran solution, roasted activated carbon was added, impregnated and stirred at room temperature for 24 hours, and then the sample was placed on a rotary evaporator to remove the solvent, and the obtained sample was dried in a drying oven at 60 °C. The dried sample is also roasted in the tube furnace under argon gas for one hour, the temperature is 450 °C, and the heating rate is 5 °C /min. After the roasting is completed, the sample is removed by the furnace after natural cooling to room temperature, which is donated as Ru/AC(450). The load capacity of Ru is 3%.

## 2. The analysis of ammonia synthesis rate

**A).** Chemical titration: The rate of ammonia synthesis was determined with Congo red as an indicator when the amount of  $\text{H}_2\text{SO}_4$  was known. The concentration of  $\text{H}_2\text{SO}_4$  used is 0.05 mol/L. Determination is to take 25  $\mu\text{L}$  of  $\text{H}_2\text{SO}_4$  and add 50  $\mu\text{L}$  of Congo red indicator to the sample tube, and then add 2 mL of deionized water, the sample tube is connected to the fixed bed reactor, record the time of indicator color change, and convert to the export ammonia rate.

**B).** Nessler's reagent spectrophotometry: The outlet ammonia is absorbed by 0.05 mol/L  $\text{H}_2\text{SO}_4$  solution, and the  $\text{NH}_4^+$  generated in the solution reacts with the Nessler's reagent to form a yellow brown complex. The absorbance of the complex is directly proportional to the content of  $\text{NH}_4^+$ . The absorbance of the complex is measured at 420 nm wavelength, and the  $\text{NH}_4^+$  content in the solution can be calculated according to the absorbance. The outlet ammonia rate is obtained.

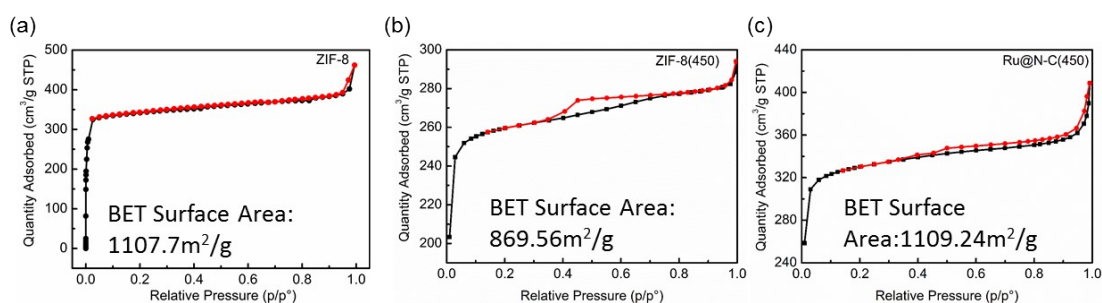


**Figure S1.** Nitrogen adsorption–desorption isotherms of ZIF-8, ZIF-8(450) and Ru@N-C(450) samples.

**Table S1.** Textural parameters of calcined ZIF-8(450) and Ru@N-C(450) samples.

Sample	$S$ (m <sup>2</sup> /g)	Pore Volume (cm <sup>3</sup> /g)	Pore Size (nm)
ZIF-8	1107.7	2.163	0.63
ZIF-8(450)	869.56	0.45	2.05
Ru@N-C(450)	1109.24	0.60	2.17

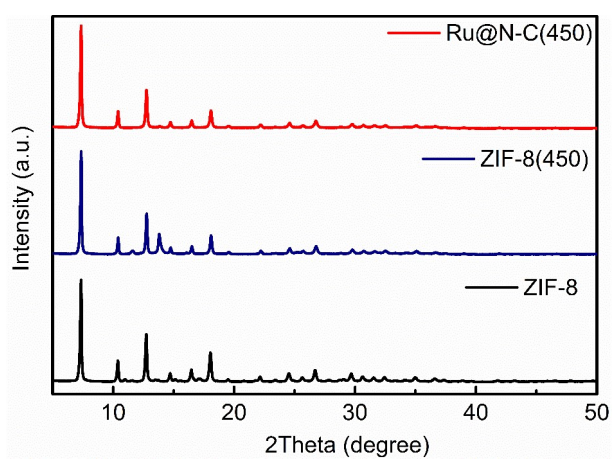


**Figure S2.** XRD patterns of ZIF-8, ZIF-8(450), and Ru@N-C(450).

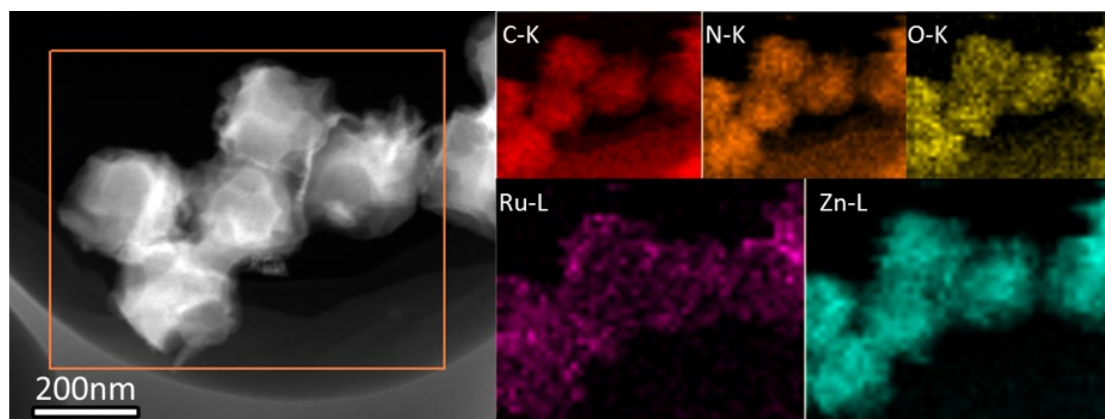


**Figure S3.** The elemental mapping of Ru@N-C(450) catalyst before reaction.

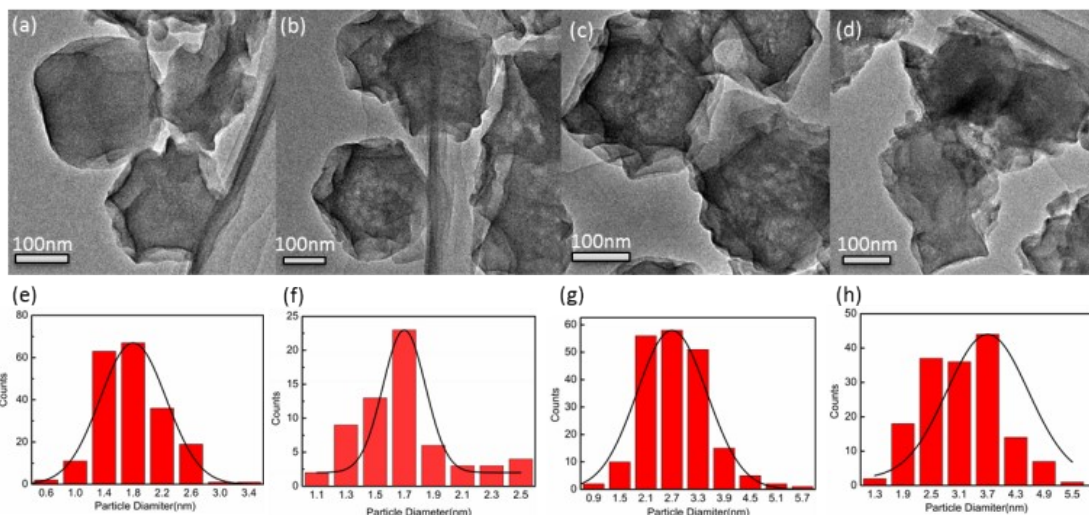


**Figure S4.** TEM images of (a) Ru@N-C(400), (b) Ru@N-C(450), (c) Ru@N-C(500), (d) Ru@N-C(900) and their corresponding Ru particle distribution histograms(e-h).

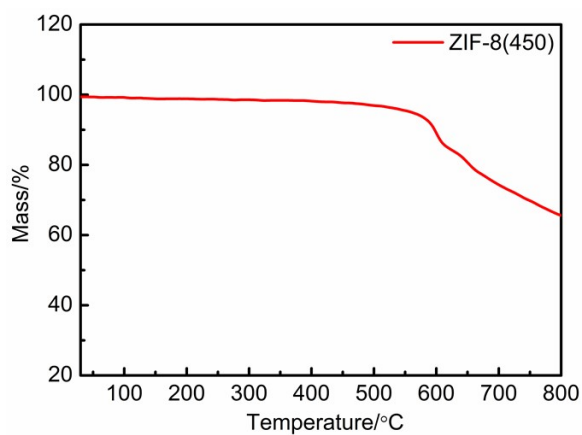


**Figure S5.** TG analysis plot of ZIF-8(450) support.

#### ZIF-8(450) catalyst:

The prepared ZIF-8 was placed in an ark and calcined in a tubular furnace at 450°C for one hour of a heating rate of 5°C /min. After the calcination, the sample was naturally cool to room temperature and then taken out and recorded as ZIF-8(450).

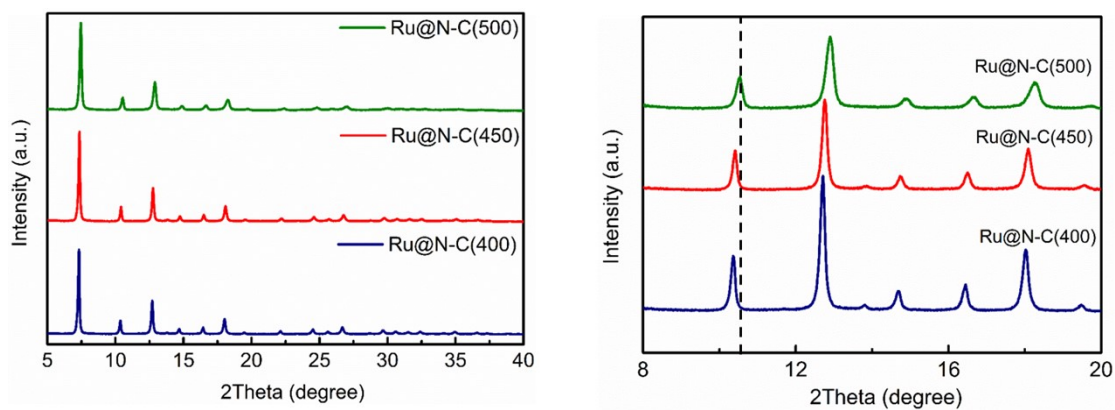


**Figure S6.** XRD patterns of Ru@N-C(400), Ru@N-C(450), and Ru@N-C(500).

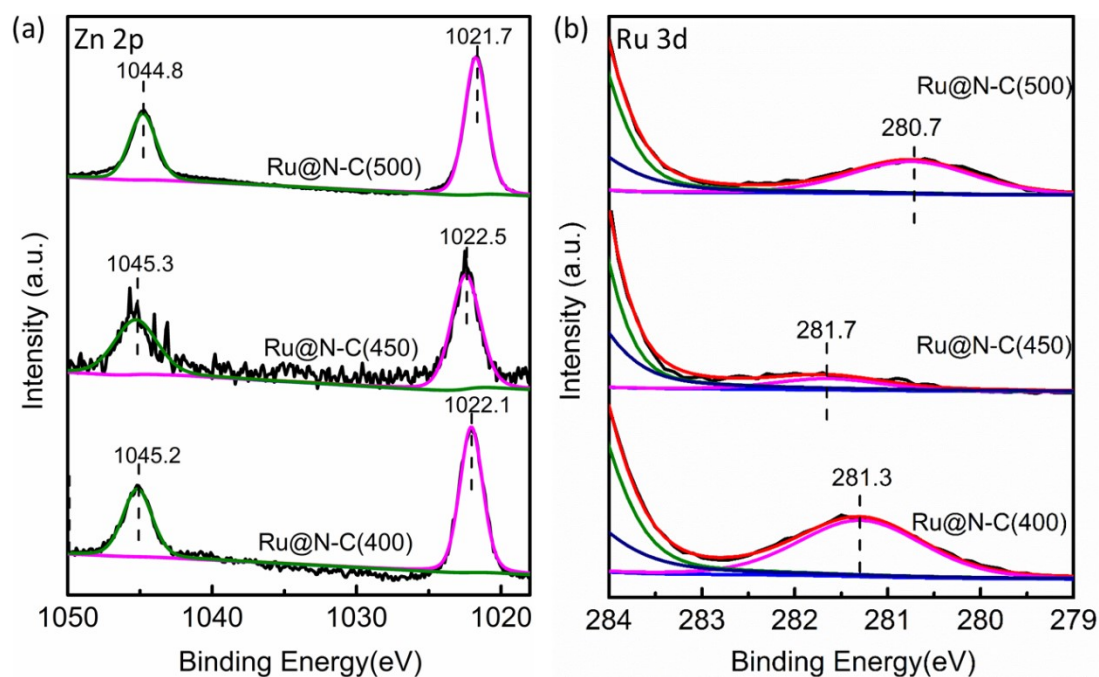


**Figure S7.** The XPS spectra of (a) Zn 2p and (b) Ru 3d in Ru@N-C(500), Ru@N-C(450) and Ru@N-C(400) catalysts.

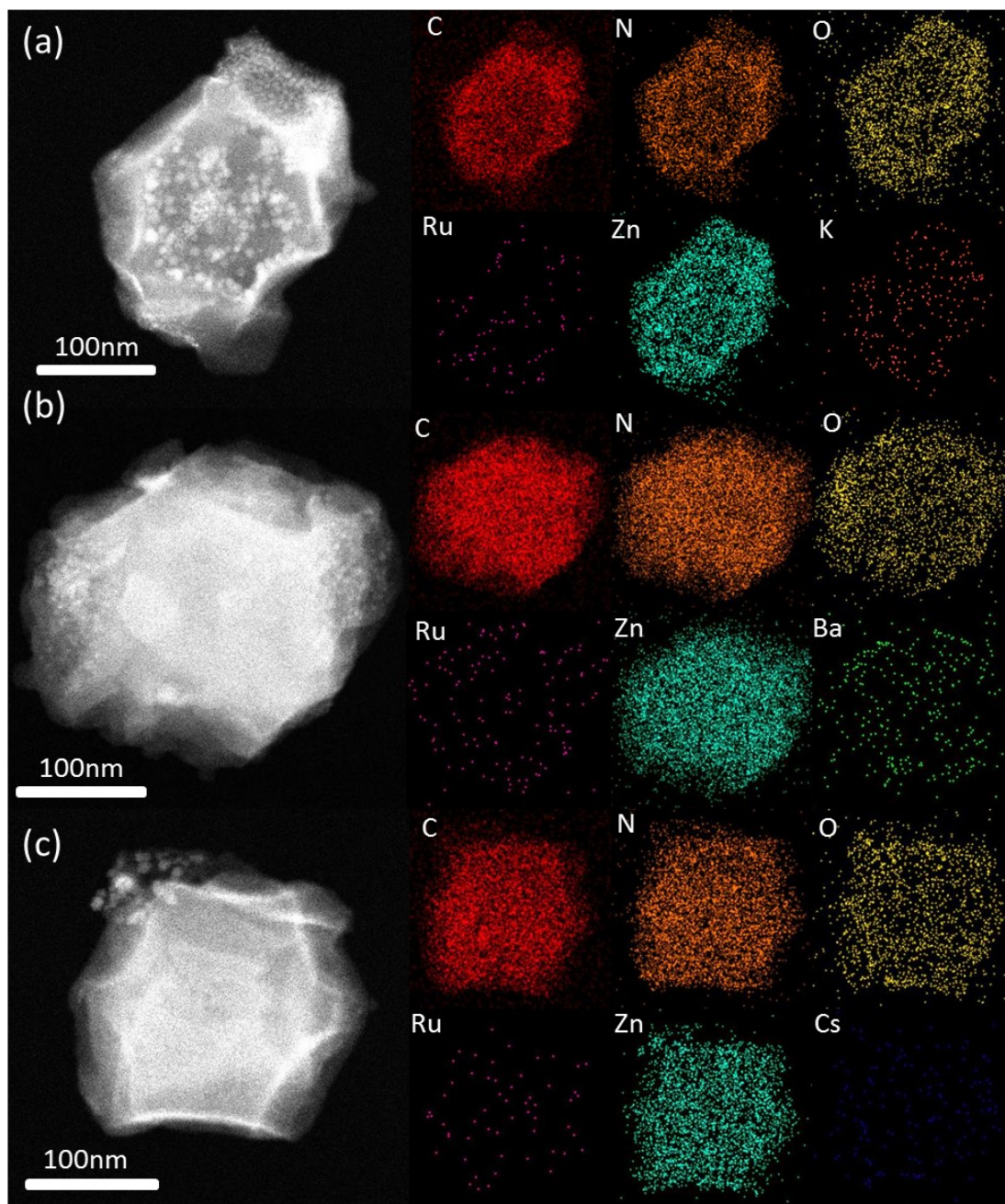


**Figure S8** The elemental mapping of (a) 2K-Ru@N-C(450), (b) 2Ba-Ru@N-C(450), (c) 2Cs-Ru@N-C(450)

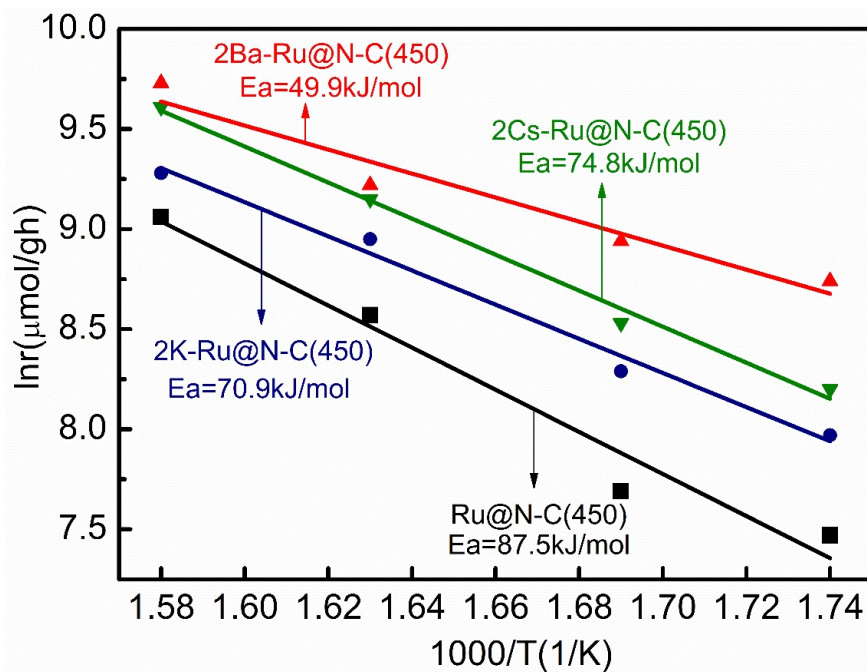


**Figure S9.** Arrhenius plots of Ru@N-C catalysts in the temperature range of 573–633 K.

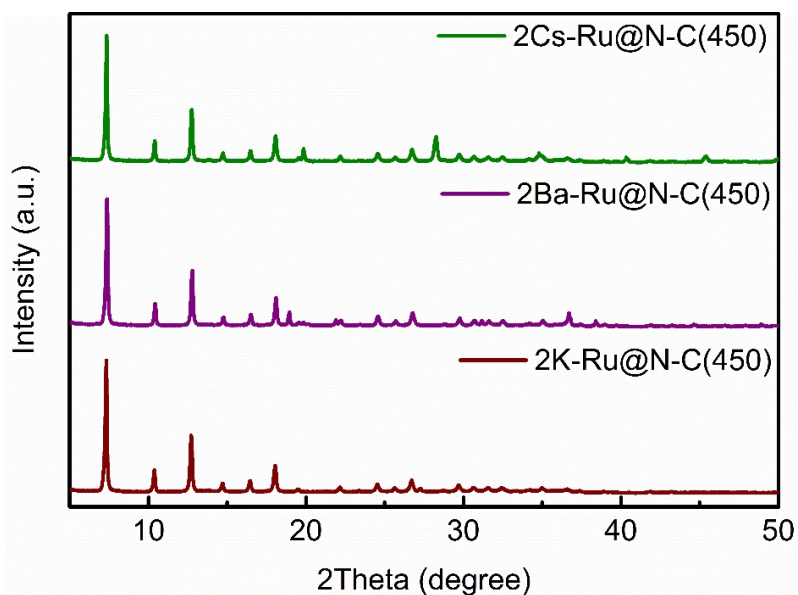


**Figure S10.** XRD patterns of 2Cs-Ru@N-C(450), 2Ba-Ru@N-C(450), and 2K-Ru@N-C(450).

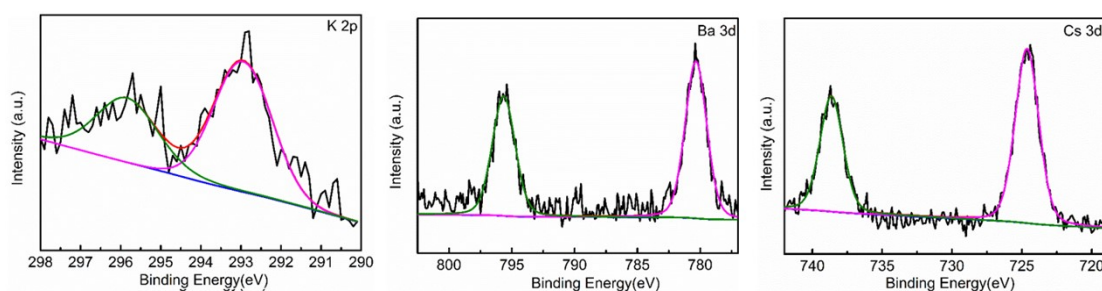


**Figure S11.** XPS spectra of K 2p, Ba 3d, and Cs 3d of 2K-Ru@N-C(450), 2Ba-Ru@N-C(450), and 2Cs-Ru@N-C(450) catalysts.

It can be noted that the Cs 3d<sup>5/2</sup> binding energy at 724.3 eV is much lower than that of Cs<sub>2</sub>O (725.2 eV) in Fig. S4. According to the previous reports [1,2], Ru nanoparticle can facilitate the decomposition of CsNO<sub>3</sub>, KNO<sub>3</sub>, and Ba(NO<sub>3</sub>)<sub>2</sub> at around 120 °C and partial Cs reduction has been observed by XAS. Thus, the Cs 3d<sup>5/2</sup> binding energy at 724.3 eV can be attributed to the partially reduced cesium (CsO<sub>x</sub>). The Ba 3d<sup>5/2</sup> binding energy at 780.4 eV is ascribed to the formation of BaO, which is in accordance with the previous report [3].

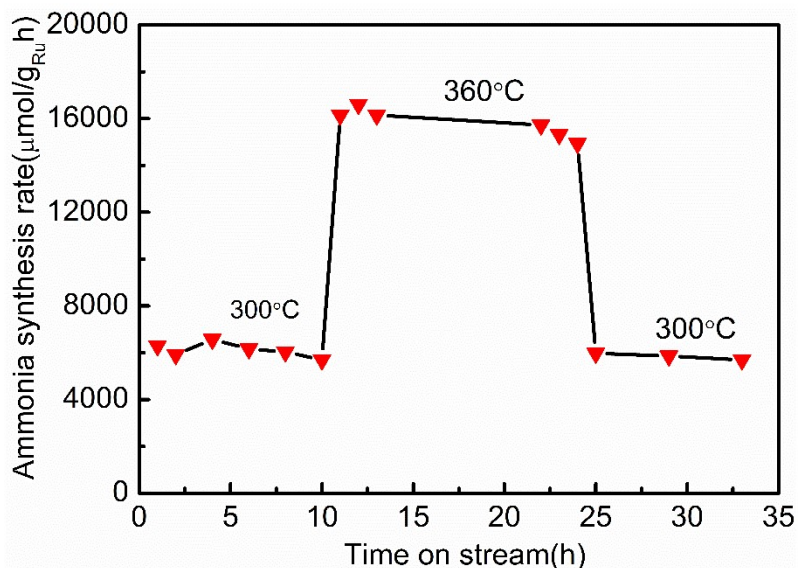


**Figure S12.** Time dependence of the catalytic activities of the 2Ba-Ru@N-C(450) catalysts. Reaction conditions: 0.5 g, N<sub>2</sub> : H<sub>2</sub> = 1 : 3, 60 mL min<sup>-1</sup>, and 1 MPa.



**Table S2.** Rate of ammonia synthesis over Ru catalysts supported on various supports.

Catalysts	Ru (wt %)	Pressure (MPa)	Temperature (°C)	Rate ( $\mu\text{mol}\cdot\text{h}^{-1}\cdot\text{g}^{-1}_{\text{Ru}}$ )	Rate ( $\mu\text{mol}\cdot\text{h}^{-1}\cdot\text{g}^{-1}_{\text{cat}}$ )	Ref.
Ru@N-C(450)	3.0	1	360	8604.2	258.1	<i>This work</i>
2Ba-Ru@N-C(450)	3.0	1	360	16817.3	504.5	<i>This work</i>
Co(0.3 %)/BaTiO <sub>3</sub>	-	5	400	-	14	4
Fe(0.4 %)/BaTiO <sub>3</sub>	-	5	400	-	200	4
Co(0.3 %)/BaTiO <sub>2.35</sub> H <sub>0.65</sub>	-	5	400	-	550	4
Ru/Eu <sub>2</sub> O <sub>3</sub> -m	3	1	400	15366	461	5
Ba-Ru/MgO	8	1	315	6037.5	483	6
Ru/spherical CeO <sub>2</sub>	4	1	400	13225	529	7
Ru Cs/MgO	5	1	300	11060	553	8
Mn <sub>4</sub> N-NaH	-	1	300	-	~50	9
Mn <sub>4</sub> N-CaH <sub>2</sub>	-	1	300	-	~400	9
Mn <sub>4</sub> N-KH	-	1	300	-	~500	9
Cs-MgO-Ru/MS	8.7	0.4	500	1095.4	92.2	10
MgO-Ru/MS	8.4	0.4	500	184.5	15.6	10
Cs-Ru/MS	5.0	0.4	500	304	15.2	10
Ru/r-Al <sub>2</sub> O <sub>3</sub>	1.9	0.1	400	421.06	8	11
Ru/CaO	1.5	0.1	350	800	12	12
Ba Ru/AC	1.0	0.1	350	1400	14	12
Ni+ Ni <sub>2</sub> Mo <sub>3</sub> N	-	0.1	400	-	15	13
Cs-Ru/r-Al <sub>2</sub> O <sub>3</sub>	2.0	0.1	315	1450	29	14
Ru/CaNH	1.8	0.1	300	2944.4	53	15

Ru/C <sub>12</sub> A <sub>7</sub> :O <sub>2</sub>	1.2	0.1	350	4916.7	59	12
CaRuSi	-	0.1	400	-	60	16
Ba-Ru/AC	1.0	0.1	400	14800	148	12
Ru/CaO	1.5	0.1	400	10533.3	158	12
CoNiMo <sub>3</sub> N	-	0.1	400	-	160	13
Ru/BaH <sub>2</sub>	10	0.1	340	2000	200	17
Ni <sub>1.7</sub> Cu <sub>0.2</sub> Mo <sub>3</sub> N	-	0.1	500	-	231	18
Ru/CaTiO <sub>3</sub>	2	0.1	400	13400	268	19
Ni <sub>2</sub> Mo <sub>3</sub> N	-	0.1	500	-	272	18
Ba-Ru/MgO	8	0.1	315	3662.5	293	6
Ru/CaNH	1.8	0.1	340	17111.1	308	15
Fe-K <sub>2</sub> O-Al <sub>2</sub> O <sub>3</sub>	-	0.1	400	-	330	16
Ni <sub>1.1</sub> Fe <sub>0.9</sub> Mo <sub>3</sub> N	-	0.1	500	-	354	19
Ni <sub>2</sub> Mo <sub>3</sub> N	-	0.1	400	-	383	13
Co <sub>3</sub> Mo <sub>3</sub> C	-	0.1	500	-	461	21
Co <sub>3</sub> Mo <sub>3</sub> N	-	0.1	500	-	489	21
Ru/C <sub>12</sub> A <sub>7</sub> :O <sub>2</sub>	1.2	0.1	400	45500	546	12
Ru/r-Al <sub>2</sub> O <sub>3</sub>	6.3	0.1	450	14650.8	923	5

#### Referance:

1. I. Rossetti, L. Sordelli, P. Ghigna, S. Pin, M. Scavini and L. Forni, EXAFS/XANES Evidence of in Situ Cesium Reduction in CsRu/C Catalysts for Ammonia Synthesis. *Inorg. Chem.*, 2011, **50**, 3757-3765.
2. I. Rossetti, F. Mangiarini and L. Forni, Promoters state and catalyst activation during ammonia synthesis over Ru/C. *Appl. Catal. A*, 2007, **323**, 219-225.
3. E. Truskiewicz, W. Raróg-Pilecka, K. Schmidt-Szałowski, S. Jodzis, E. Wilczkowska, D. Łomot, Z. Kaszkur, Z. Karpiński and Z. Kowalczyk, Barium-promoted Ru/carbon catalyst for ammonia synthesis: State of the system when operating. *J. Catal.*, 2009, **265**, 181-190.
4. Y. Tang, Y. Kobayashi, N. Masuda, Y. Uchida, H. Okamoto, T. Kageyama, S. Hosokawa, F. Loyer, K. Mitsuahara, K. Yamanaka, et al, Metal-Dependent Support Effects of Oxyhydride-Supported Ru, Fe, Co Catalysts for Ammonia Synthesis. *Met. Adv. Energy. Mater.*, 2018, **8**, 1801772.

5. A. Miyazaki, I. Balint, K. I. Aika and Y. Nakano, Preparation of High Activity Catalyst for Ammonia Synthesis by Supporting Well-Defined Ru Nanoparticles on  $\gamma$ -Al<sub>2</sub>O<sub>3</sub>. *Chemistry Letters*, 2003, **12**, 1332-1333.
6. Z. You, K. Inazu, K. I. Aika and T. Baba, Electronic and structural promotion of barium hexaaluminate as a ruthenium catalyst support for ammonia synthesis. *Journal of Catalysis*, 2007, **251**, 321-331.
7. Z. Ma, S. Zhao, X. Pei, X. Xiong and B. Hu, New insights into the support morphology-dependent ammonia synthesis activity of Ru/CeO<sub>2</sub> catalysts. *Catal. Sci. Technol.*, 2017, **7**, 191-199.
8. K. Kishida, M. Kitano, M. Sasase, P. V. Sushko, H. Abe, Y. Niwa, K. Ogasawara, T. Yokoyama and H. Hosono, Air-Stable Calcium Cyanamide-Supported Ruthenium Catalyst for Ammonia Synthesis and Decomposition. *ACS Appl. Energy Mater.*, 2020, **3**, 6573-6582.
9. F. Chang, Y. Guan, X. Chang, J. Guo, P. Wang, W. Gao, G. Wu, J. Zheng, X. Li and P. Chen, Alkali and Alkaline Earth Hydrides-Driven N<sub>2</sub> Activation and Transformation over Mn Nitride Catalyst. *J. Am. Chem. Soc.*, 2018, **140**, 14799-14806.
10. J. Ding, L. Wang, P. Wu, A. Li, W. Li, C. Stampfl, X. Liao, B. S. Haynes, X. Han and J. Huang, Confined Ru Nanocatalysts on Surface to Enhance Ammonia Synthesis: An In situ ETEM Study. *ChemCatChem.*, 2020, **13**, 534-538.
11. S. Murata and K. Aika, Preparation and characterization of chlorine-free ruthenium catalysts and the promoter effect in ammonia synthesis.: 1. An alumina-supported ruthenium catalyst. *Journal of Catalysis*, 1992, **136**, 110-117.
12. M. Kitano, Y. Inoue, Y. Yamazaki, F. Hayashi, S. Kanbara, S. Matsuishi, T. Yokoyama, S. W. Kim, M. Hara and H. Hosono, Ammonia synthesis using a stable electride as an electron donor and reversible hydrogen store. *Nat. Chem.*, 2012, **4**, 934-940.
13. N. Bion, F. Can, J. Cook, JSJ. Hargreaves, A. L. Hector, W. Levason, A. R. McFarlane, M. Richard and K. Sardar, The role of preparation route upon the ambient pressure ammonia synthesis activity of Ni<sub>2</sub>Mo<sub>3</sub>N. *Appl. Catal. A*. 2015, **504**, 44-50.
14. S. Murata and K. Aika, Preparation and characterization of chlorine-free ruthenium catalysts and the promoter effect in ammonia synthesis.: 1. An alumina-supported ruthenium catalyst. *Journal of Catalysis*, 1992, **136**, 118-125.
15. M. Kitano, Y. Inoue, H. Ishikawa, K. Yamagata, T. Nakao, T. Tada, S. Matsuishi, T. Yokoyama, M. Hara and H. Hosono, Essential role of hydride ion in ruthenium-based ammonia synthesis catalysts. *Chem. Sci.*, 2016, **7**, 4036-4043.
16. Y. Gong, J. Wu, M. Kitano, J. Wang, T. N. Ye, J. Li, Y. Kobayashi, K. Kishida, H. Abe, Y. Niwa, et al., Ternary intermetallic LaCoSi as a catalyst for N<sub>2</sub> activation. *Nat. Cat.*, 2018, **1**, 178-185.
17. J. Wu, J. Li, Y. Gong, M. Kitano, T. Inoshita and H. Hosono, Intermetallic Electride Catalyst as a Platform for Ammonia Synthesis. *Angew. Chem. Int. Ed.*, 2019, **58**, 825-829.
18. M. Hattori, T. Mori, T. Arai, Y. Inoue, M. Sasase, T. Tada, M. Kitano, T. Yokoyama, M. Hara and H. Hosono, Enhanced Catalytic Ammonia Synthesis with Transformed BaO. *ACS. Catal.*, 2018, **8**, 10977-10984.
19. S. Al Sobhi, JSJ. Hargreaves, A. L. Hector and S. Laassiri, Citrate-gel preparation and ammonia synthesis activity of compounds in the quaternary (Ni,M)<sub>2</sub>Mo<sub>3</sub>N (M = Cu or Fe) systems. *Dalton Trans*, 2019, **48**, 16786-16792.
20. Y. Horiuchi, G. Kamei, M. Saito and M. Matsuoka, Development of Ruthenium-loaded Alkaline-earth Titanates as Catalysts for Ammonia Synthesis. *Chem. Lett.*, 2013, **42**, 1282-1284.
21. I. AlShibane, A. Daisley, JSJ. Hargreaves, A. L. Hector, S. Laassiri, J. L. Rico and R. I. Smith, The Role of

Composition for Cobalt Molybdenum Carbide in Ammonia Synthesis. ACS. Sustainable. Chem. Eng., 2017, 5, 9214-9222.